

Ambiguity function display: an improved coherent processor

Robert J. Marks II, John F. Walkup, and Thomas F. Krile

A coherent optical processor for displaying a signal's ambiguity function is described. The required time delay is realized by 45° rotations of two identical input transparencies and the Doppler shift by a 1-D Fourier transformation. The entire ambiguity function is displayed in the output (Doppler shift-time delay) plane. Examples of the optically computed ambiguity function for single and double pulse signals are shown to be in excellent agreement with theory. Advantages of this approach over other schemes and possible extension to real time processing are also discussed.

I. Introduction

The ambiguity function, first introduced by Woodward,¹ has been applied in radar in predicting the capability of a given signal to determine simultaneously the range and velocity of a target. The range is determined by the time delay τ and the velocity by the Doppler shift ν . The ambiguity function for a given real-valued signal $f(t)$ is

$$\chi(\nu, \tau) = \int_{-\infty}^{\infty} f(t)f(t - \tau) \exp(-j2\pi\nu t) dt, \quad (1)$$

In optics, Papoulis has employed the ambiguity function in analyzing diffraction phenomena.²

In this paper, we describe a rather easily implemented coherent processor capable of generating the ambiguity function in magnitude. A similar, yet somewhat more elaborate, scheme for generating $\chi(\nu, \tau)$ in both magnitude and phase is given in the Appendix. Such a scheme, for example, would need to be utilized when further coherent processing of the ambiguity function is required.

Cutrona *et al.*^{3,4} and Preston⁵ have proposed a coherent ambiguity function processor⁶ which utilizes multiple channels to display the ambiguity function for discrete values of τ . The scheme of Casasent *et al.*⁷ generates 1-D slices of the ambiguity function in the (ν, τ) plane. Similar 1-D displays have also been electronically produced.⁸ Our method, as described in the following sections, (1) displays $|\chi(\nu, \tau)|^2$ in a continuous (rather than quantized) form over the entire (ν, τ) plane, (2) has the capacity for extension to real time processing, and (3) is easily implemented.

II. Geometrical Interpretation

On the (t, τ) plane, a function $f(t)$ takes on the 1-D nature exemplified in Fig. 1(a). Upon rotating this function counterclockwise about the origin through an angle θ , we generate the function [Fig. 1(b)]

$$f(t \cos \theta + \tau \sin \theta). \quad (2)$$

Thus, for a rotation of 45°, we obtain $f[(t + \tau)/\sqrt{2}]$, and for a rotation of -45°, we obtain $f[(t - \tau)/\sqrt{2}]$. Consider, then, multiplying these two functions [Fig. 1(c)] and performing a Fourier transformation with respect to t :

$$\int_{-\infty}^{\infty} f\left(\frac{t + \tau}{\sqrt{2}}\right) f\left(\frac{t - \tau}{\sqrt{2}}\right) \exp(-j2\pi\nu t) dt, \quad (3)$$

where ν is the frequency variable associated with t . Upon making the variable substitution $t' = (t + \tau)/\sqrt{2}$, Eq. (3) becomes a scaled version of the ambiguity function of Eq. (1):

$$\begin{aligned} \sqrt{2} \exp(j2\pi\nu\tau) \int_{-\infty}^{\infty} f(t')f(t' - \sqrt{2}\tau) \exp[-j2\pi(\sqrt{2}\nu)t'] dt' \\ = \sqrt{2}\chi(\sqrt{2}\nu, \sqrt{2}\tau) \exp(j2\pi\nu\tau). \end{aligned} \quad (4)$$

Thus, apart from a multiplicative phase term, we may generate a scaled version of the ambiguity function by representing the time delay by simple 45° rotations and the Doppler shift by an appropriate 1-D Fourier transformation.

III. Implementation Scheme

A processor capable of performing a 1-D Fourier transform is given in Fig. 2. The field amplitude $U(\nu, \tau)$ in plane P_2 is related to the coherently illuminated transmittance $s(t, \tau)$ in plane P_1 by

$$U(\nu, \tau) = \exp(-j2\pi\lambda f\nu^2) \int_{-\infty}^{\infty} s(t, -\tau) \exp(-j2\pi\nu t) dt, \quad (5)$$

where λ is the wavelength of the spatially coherent il-

T. F. Krile is with Rose-Hulman Institute of Technology, Department of Electrical Engineering, Terre Haute, Indiana 47803; the other authors are with Texas Tech University, Department of Electrical Engineering, Lubbock, Texas 79409.

Received 2 August 1976.

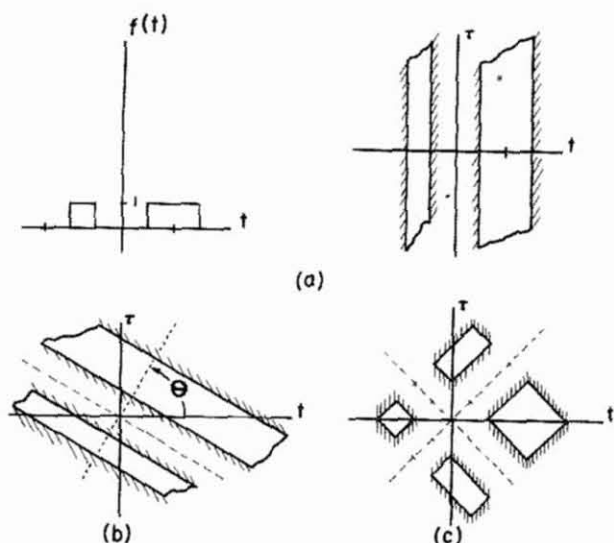


Fig. 1. (a) A function $f(t)$ in time and in the (t, τ) plane. (b) By rotating $f(t)$ counterclockwise an angle of θ about the origin of the (t, τ) plane, we generate $f(t \cos \theta + \tau \sin \theta)$. (c) The function $f[(t + \tau)/\sqrt{2}]f[(t - \tau)/\sqrt{2}]$ in the (t, τ) plane.

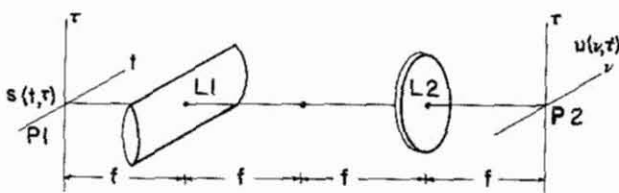


Fig. 2. A coherent processor for ambiguity function display. Both the lenses have focal length f . Fourier transformation is performed in the horizontal direction and imaging in the vertical direction.

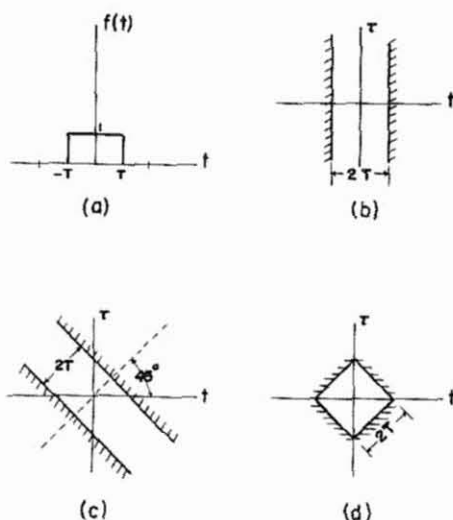


Fig. 3. A single pulse (a) in time, (b) in the (t, τ) plane, (c) rotated 45° on the (t, τ) plane to form $f[(t + \tau)/\sqrt{2}]$, (d) the product of two pulses rotated 45° and -45° on the (t, τ) plane to form $f[(t + \tau)/\sqrt{2}]f[(t - \tau)/\sqrt{2}]$.

illumination, f is the focal length of both lenses L_1 and L_2 , and the spatial frequency ν is related to the horizontal displacement x_2 on plane P_2 by⁹

$$\nu = x_2/\lambda f. \quad (6)$$

Consider, then, placing two identical 1-D transparencies of $f(t)$ in plane P_1 , each rotated 45° in such a manner as to form the product

$$s(t, \tau) = f\left(\frac{t + \tau}{\sqrt{2}}\right) f\left(\frac{t - \tau}{\sqrt{2}}\right). \quad (7)$$

The corresponding field amplitude in plane P_2 [from Eq. (5)] is then given by

$$U(\nu, \tau) = \exp(-j2\pi\lambda f\nu^2) \int_{-\infty}^{\infty} f\left(\frac{t - \tau}{\sqrt{2}}\right) f\left(\frac{t + \tau}{\sqrt{2}}\right) \times \exp(-j2\pi\nu t) dt \\ = \sqrt{2} \exp[-j2\pi\nu(\tau + \lambda f\nu)] \\ \times \int_{-\infty}^{\infty} f(t')f(t' - \sqrt{2}\tau) \exp[-j2\pi(\sqrt{2}\nu)t'] dt', \quad (8)$$

where, as before, we have made the change of variable $t' = (t + \tau)/\sqrt{2}$. The intensity distribution associated with Eq. (8) is immediately recognized as a scaled version of the squared modulus of the ambiguity function¹⁰:

$$I(\nu, \tau) = |U(\nu, \tau)|^2 \\ = 2|\chi(\sqrt{2}\nu, \sqrt{2}\tau)|^2. \quad (9)$$

IV. Experimental Results

To evaluate the performance of the proposed processor, the ambiguity functions for a single and double pulse signal are evaluated analytically and compared to the corresponding optical system outputs. In practice, the processor output is magnified by conventional means for observation and photographic purposes.

A. Single Pulse

For a single pulse [Fig. 3(a)], we may write

$$f(t) = \text{rect}(t/2T), \quad (10)$$

where $2T$ is the pulse duration, and

$$\text{rect}(t) \triangleq \begin{cases} 1; & |t| \leq 1/2, \\ 0; & |t| > 1/2. \end{cases}$$

The geometric interpretations of $f(t)$, $f[(t + \tau)/\sqrt{2}]$, and $f[(t + \tau)/\sqrt{2}]f[(t - \tau)/\sqrt{2}]$ are shown in Figs. 3(b), 3(c), and 3(d), respectively.

Substituting Eq. (10) into Eq. (1) followed by evaluation yields the ambiguity function

$$\chi(\nu, \tau) = \begin{cases} (2T - |\tau|) \text{sinc}\nu(2T - |\tau|) \exp(-j\pi\nu\tau); & |\tau| \leq 2T \\ 0; & |\tau| \geq 2T, \end{cases} \quad (11)$$

where

$$\text{sinc}\nu \triangleq (\sin \pi\nu)/\pi\nu.$$

The corresponding output intensity is

$$|\chi(\nu, \tau)|^2 = \begin{cases} (2T - |\tau|)^2 \text{sinc}^2\nu(2T - |\tau|); & |\tau| \leq 2T \\ 0; & |\tau| \geq 2T. \end{cases} \quad (12)$$

For purposes of identification, it is instructive to examine the locus of points where the ambiguity func-

tion is identically zero. From Eq. (12), this zero locus may easily be shown to be

$$\nu = n/(2T - |\tau|); |\tau| \leq 2T, \quad (13)$$

where n is any nonzero integer. The piecewise hyperbolic nature of these curves is shown in Fig. 4.

The ambiguity function for a single pulse is generated by appropriately rotating two identical thin slits in plane P_1 of the coherent optical processor of Fig. 2. The result is shown in Fig. 5. As can be seen, the coherent processor output compares quite nicely with the theoretical result in Fig. 4. A 3-D computer graph of the corresponding ambiguity function modulus may be found in Fig. 6.6 of Rihaczek.¹¹

B. For a Double Pulse

For a double pulse [Fig. 6(a)], we write

$$f(t) = \text{rect}[(t + 2T)/2T] + \text{rect}[(t - 2T)/2T], \quad (14)$$

where, for convenience, the pulse separation $2T$ has been chosen to be equal to each pulse width. The geometrical interpretation of $f[(t - \tau)/\sqrt{2}]f[(t + \tau)/\sqrt{2}]$ is shown in Fig. 6(b). The ambiguity function associated with the double pulse is

$$\chi(\nu, \tau) = \begin{cases} 2(2T - |\tau|) \text{sinc}_\nu(2T - |\tau|) \cos(4\pi T\nu) \exp(-j\pi\tau\nu); & |\tau| \leq 2T \\ -(2T - |\tau|) \text{sinc}_\nu(2T - |\tau|) \exp(-j\pi\tau\nu); & 2T \leq |\tau| \leq 4T \\ (6T - |\tau|) \text{sinc}_\nu(6T - |\tau|) \exp(-j\pi\tau\nu); & 4T \leq |\tau| \leq 6T \\ 0 & |\tau| \geq 6T. \end{cases} \quad (15)$$

The corresponding output intensity is

$$|\chi(\nu, \tau)|^2 = \begin{cases} 4(2T - |\tau|)^2 \text{sinc}_\nu^2(2T - |\tau|) \cos^2(4\pi T\nu); & |\tau| \leq 2T \\ (2T - |\tau|)^2 \text{sinc}_\nu^2(2T - |\tau|); & 2T \leq |\tau| \leq 4T \\ (6T - |\tau|)^2 \text{sinc}_\nu^2(6T - |\tau|); & 4T \leq |\tau| \leq 6T \\ 0 & |\tau| \geq 6T. \end{cases} \quad (16)$$

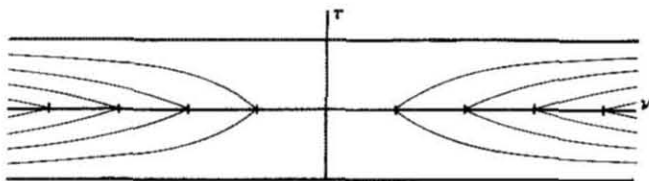


Fig. 4. Zero locus plot of the ambiguity function of a single pulse.

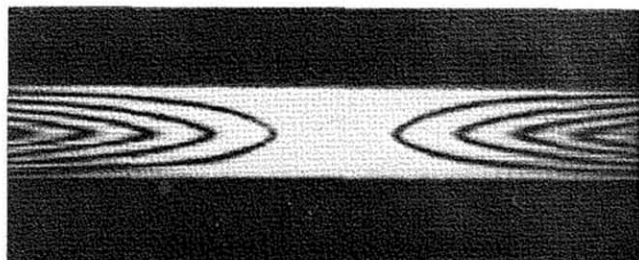


Fig. 5. The ambiguity function (modulus squared) display for a single pulse, as generated by the coherent processor of Fig. 2.

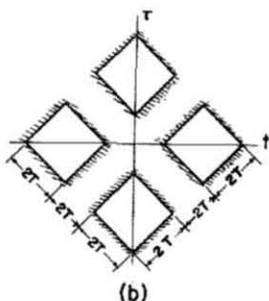
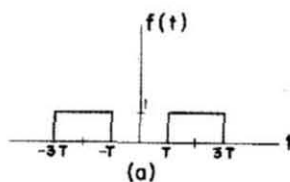


Fig. 6. (a) A double pulse. (b) The corresponding function $f[(t + \tau)/\sqrt{2}]f[(t - \tau)/\sqrt{2}]$ in the (t, τ) plane.

The equations describing the zero-value loci are easily shown to be

$$\begin{aligned} \nu &= (2m + 1)/8T; |\tau| \leq 2T, \\ \nu &= n/(|\tau| - 2T); |\tau| \leq 4T, \\ \nu &= n/(6T - |\tau|); 4T \leq |\tau| \leq 6T, \end{aligned} \quad (17)$$

where m is any integer, and, as before, n is any nonzero integer. An illustration of these zero-value loci is offered in Fig. 7.

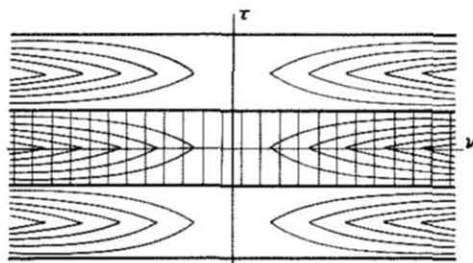


Fig. 7. Zero locus plot of the ambiguity function of a double pulse.

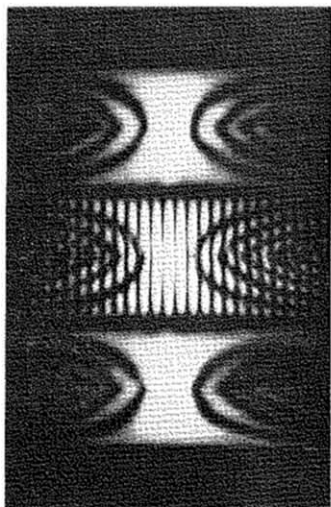


Fig. 8. The ambiguity function (modulus squared) display for a double pulse as generated by the coherent processor of Fig. 2.

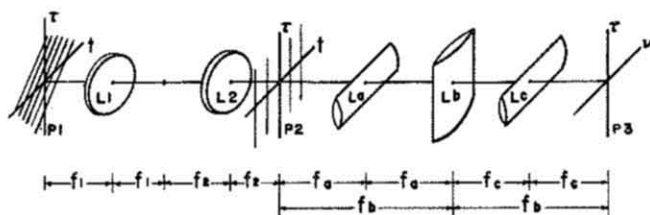


Fig. 9. Coherent processor for generating the ambiguity function in phase and amplitude. Scaling lenses L_1 and L_2 have a focal length relation $f_1 = \sqrt{2}f_2$.

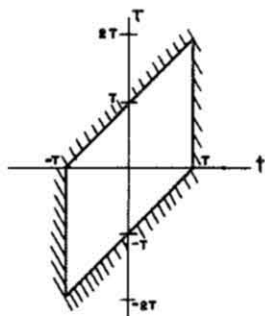


Fig. 10. The product $f(t)f(t - \tau)$ in the (t, τ) plane for the single pulse of Fig. 3(a).

By appropriately placing two identical double slits in plane P_1 of the coherent processor, the ambiguity function for the double pulse is generated. The result, shown in Fig. 8, again compares quite favorably with the theory.

V. Conclusions

We have demonstrated a rather easily implemented coherent optical processor capable of computing a signal's ambiguity function. The required time delayed signal results from 45° rotations of the transmitted signal. The Doppler shift variable is obtained by an appropriate 1-D Fourier transformation. The entire (ν, τ) plane is displayed at once, and no motion is required. The processor output demonstrates good agreement with theoretical results.

The ambiguity function processor could easily be extended to real time by utilizing two synchronized (1-D) electrical-to-optical transducers to generate the two required identical radar signals.

As a final note, we observe that the scheme we propose assumes that $f(t)$ is real valued. If, in fact, $f(t)$ is complex, we need to generate $f^*(t - \tau)$ in the integrand of Eq. (1) in order to generate $\chi(\nu, \tau)$ properly. Some additional work appears needed for the case of a general complex-valued $f(t)$.

The authors express their appreciation to Steven V. Bell, Gary Froehlich, Richard W. Thomas, Jr., John A. Vincent, and Kingsley Wong for their assistance in the preparation of this paper.

This research was supported by the Air Force Office of Scientific Research, Air Force Systems Command, USAF, under grant AFOSR-75-2855A.

Appendix

A coherent processor capable of computing $\chi(\nu, \tau)$ in both phase and amplitude to within a proportionality constant is shown in Fig. 9. In plane P_1 , we place the transmittance $f[(\tau - t)/\sqrt{2}]$ which is formed by the previously discussed 45° rotation of $f(t)$, followed by coordinate reversal [rotating $f[(t - \tau)/\sqrt{2}]$ 180° degrees about both the t and τ axes]. The scaling lenses L_1 and L_2 have respective focal lengths related by $f_1 = \sqrt{2}f_2$. The field amplitude incident on the left of plane P_2 is the desired $f(t - \tau)$. This will multiply the transmittance $f(t)$ in plane P_2 to give immediately to the right of P_2 the field amplitude $f(t)f(t - \tau)$. The geometrical interpretation of this product in the (t, τ) plane, for the case of a single pulse, is shown in Fig. 10.

With reference to Eq. (1), it remains to perform a Fourier transformation with respect to t . This is accomplished with cylindrical lenses L_a , L_b , and L_c which have respective focal lengths of

$$2f_a = f_b = 2f_c.$$

One sees that, from plane P_2 to P_3 , imaging is performed in the vertical direction by L_a and L_c while Fourier transformation is independently performed in the horizontal direction by L_b . Thus, the field amplitude, $U(\nu, \tau)$, in plane P_3 is a scaled version of the ambiguity function

$$\begin{aligned} U(\nu, \tau) &= \int_{-\infty}^{\infty} f(t)f(t - \tau) \exp(-j2\pi\nu t) dt \\ &= \chi(\nu, \tau), \end{aligned}$$

where ν is related to the horizontal displacement x_3 in P_3 by $\nu = x_3/\lambda_f$.

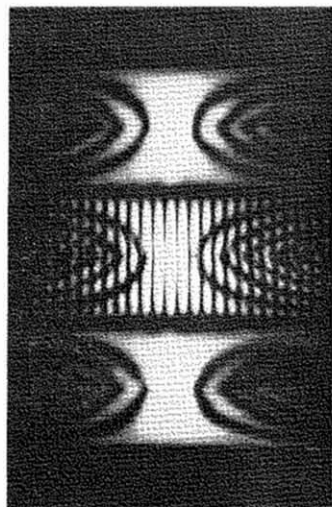


Fig. 8. The ambiguity function (modulus squared) display for a double pulse as generated by the coherent processor of Fig. 2.

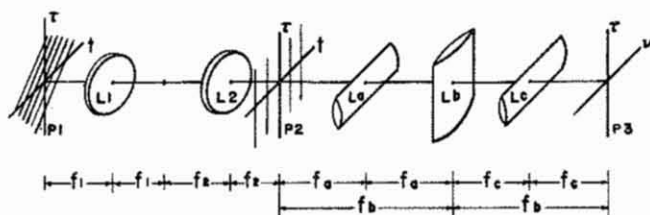


Fig. 9. Coherent processor for generating the ambiguity function in phase and amplitude. Scaling lenses L_1 and L_2 have a focal length relation $f_1 = \sqrt{2}f_2$.

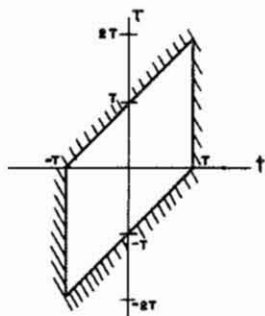


Fig. 10. The product $f(t)f(t - \tau)$ in the (t, τ) plane for the single pulse of Fig. 3(a).

By appropriately placing two identical double slits in plane P_1 of the coherent processor, the ambiguity function for the double pulse is generated. The result, shown in Fig. 8, again compares quite favorably with the theory.

V. Conclusions

We have demonstrated a rather easily implemented coherent optical processor capable of computing a signal's ambiguity function. The required time delayed signal results from 45° rotations of the transmitted signal. The Doppler shift variable is obtained by an appropriate 1-D Fourier transformation. The entire (ν, τ) plane is displayed at once, and no motion is required. The processor output demonstrates good agreement with theoretical results.

The ambiguity function processor could easily be extended to real time by utilizing two synchronized (1-D) electrical-to-optical transducers to generate the two required identical radar signals.

As a final note, we observe that the scheme we propose assumes that $f(t)$ is real valued. If, in fact, $f(t)$ is complex, we need to generate $f^*(t - \tau)$ in the integrand of Eq. (1) in order to generate $\chi(\nu, \tau)$ properly. Some additional work appears needed for the case of a general complex-valued $f(t)$.

The authors express their appreciation to Steven V. Bell, Gary Froehlich, Richard W. Thomas, Jr., John A. Vincent, and Kingsley Wong for their assistance in the preparation of this paper.

This research was supported by the Air Force Office of Scientific Research, Air Force Systems Command, USAF, under grant AFOSR-75-2855A.

Appendix

A coherent processor capable of computing $\chi(\nu, \tau)$ in both phase and amplitude to within a proportionality constant is shown in Fig. 9. In plane P_1 , we place the transmittance $f[(\tau - t)/\sqrt{2}]$ which is formed by the previously discussed 45° rotation of $f(t)$, followed by coordinate reversal [rotating $f[(t - \tau)/\sqrt{2}]$ 180 degrees about both the t and τ axes]. The scaling lenses L_1 and L_2 have respective focal lengths related by $f_1 = \sqrt{2}f_2$. The field amplitude incident on the left of plane P_2 is the desired $f(t - \tau)$. This will multiply the transmittance $f(t)$ in plane P_2 to give immediately to the right of P_2 the field amplitude $f(t)f(t - \tau)$. The geometrical interpretation of this product in the (t, τ) plane, for the case of a single pulse, is shown in Fig. 10.

With reference to Eq. (1), it remains to perform a Fourier transformation with respect to t . This is accomplished with cylindrical lenses L_a, L_b , and L_c which have respective focal lengths of

$$2f_a = f_b = 2f_c.$$

One sees that, from plane P_2 to P_3 , imaging is performed in the vertical direction by L_a and L_c while Fourier transformation is independently performed in the horizontal direction by L_b . Thus, the field amplitude, $U(\nu, \tau)$, in plane P_3 is a scaled version of the ambiguity function

$$U(\nu, \tau) = \int_{-\infty}^{\infty} f(t)f(t - \tau) \exp(-j2\pi\nu t) dt \\ = \chi(\nu, \tau),$$

where ν is related to the horizontal displacement x_3 in P_3 by $\nu = x_3/\lambda_f$.

This ambiguity function processor, which is more elaborate than that shown in Fig. 2, need be used only when the ambiguity function's phase is required in addition to its magnitude.

References

1. P. W. Woodward, *Probability and Information Theory, With Applications to Radar* (Pergamon, Oxford, 1963).
 2. A. Papoulis, *J. Opt. Soc. Am.* **64**, 779 (1974).
 3. L. J. Cutrona, E. N. Leith, C. J. Palermo, and L. J. Porcello, *IRE Trans. Inf. Theory* **IT-6**, 386 (1960).
 4. L. J. Cutrona, in *Optical and Electro-Optical Information Processing*, J. T. Tippet *et al.*, Eds. (MIT Press, Cambridge, Mass., 1965).
 5. K. Preston, *Coherent Optical Computers* (McGraw-Hill, New York, 1972).
 6. The ambiguity function processors in Refs. 4, 5 and 7, 8 should rigorously be called uncertainty function processors in that they are only capable of displaying the uncertainty function $|\chi(\nu, \tau)|$. Following this precedent, we herein refer to both $\chi(\nu, \tau)$ and $|\chi(\nu, \tau)|$ as the ambiguity function. The actual function to which reference is made is clear in the context of the paper.
 7. D. Casasent and F. Casasayas, *Appl. Opt.* **14**, 1364 (1975).
 8. M. C. Bartlett, L. W. Couch, and R. C. Johnson, *Proc. IEEE* **63**, 1625 (1975).
 9. J. W. Goodman, *Introduction to Fourier Optics* (McGraw-Hill, New York, 1968).
 10. The squared modulus of the ambiguity function is sometimes also referred to as the ambiguity function.
 11. A. W. Rihaczek, *Principles of High Resolution Radar* (McGraw-Hill, New York, 1969).
-